JOURNAL OF CATALYSIS 86, 32–47 (1984)

The Influence of Intraparticle Mass Transfer on the Activity of a Gel-Form Polymer-Bound Transition Metal Catalyst

JOHN B. ROUCIS AND JOHN G. EKERDT

Department of Chemical Engineering, University of Texas, Austin, Texas 78712

Received April 21, 1983; revised October 6, 1983

A mathematical model was developed to investigate the influence of substrate intraparticle mass transport limitations on the hydrogenation rate of cyclohexene and cyclooctene at 25 to 50°C, 1 atm hydrogen pressure, over $RhCl(PPh_3)_3$ bound to polystyrene–divinylbenzene (DVB) polymer beads. Initial solute concentrations of ca. 0.16 *M* were used for the reaction rate studies. Intraparticle transport limitations were determined to be negligible within the 200–400 mesh, 1, 2, and 3% DVB catalyst beads under the reaction conditions employed. Changes in the reduction rate of cyclooctene relative to cyclohexene were not caused by differences in intraparticle diffusion rates. Alterations in selectivity were related to the catalyst bead swelling ratio implying that steric effects induced by the presence of the polymer support in the vicinity of active rhodium affected intrinsic activity. Intrinsic activity was found to depend on polymer crosslink density and functionalized swelling ratio. Studies of the equilibrium distribution of substrate between the solvent-swollen polymer phase and the surrounding bulk phase solution indicated that the substrate distributed uniformly for the low DVB crosslinked beads used. The mathematical model was used to study the measured reaction rate for an intraparticle mass transport influenced system: hydrogenation of cyclohexene and cyclooctene over Wilkinson's complex supported on 18–20 mesh, 3% DVB polymer beads.

I. INTRODUCTION

Many transition metal complex catalysts have been attached to crosslinked polymer supports. The subject has been reviewed in the literature (*1–8*). The review authors have discussed the relative advantages and disadvantages of supporting transition metal complex catalysts on insoluble organic supports. Polymer-bound complexes have been observed to exhibit catalytic properties similar to their homogeneous analogs. An important advantage of polymer-supported catalysts over the homogeneous complex is the ability to separate them from the reaction mixture by filtration. This feature would allow utilization of polymer-supported complex catalysts in fixed-bed reactors.

However, difficulties with polymer-bound catalyst systems have been identified. These difficulties include changes in activity and selectivity due to the altered ligand environment (*9, 10*); steric constraints imposed by the presence of the polymer structure in the vicinity of the attached complex (*8, 10, 11*); reduced activity due to the thermodynamic exclusion of reactant molecules from the solvent-swollen polymer support phase (*14*); and intraparticle mass transport effects on the reaction rate since the reactants must diffuse through the solvent-swollen polymer matrix to reach active complexes therein (*8, 9, 11–16*).

Gates and co-workers (*17, 18*) have investigated the dependence of catalytic activity on polymer support structure for a macroporous, sulfonated poly(styrene-ethylvinyl benzene-divinylbenzene) resin catalyst. They related the observed catalytic activity to polymer swelling and reactant transport effects. For vapor phase reactants, both polymer swelling and micropore diffusion influenced the reaction rate. Diffusion effects within the solvent channels were negligible.

This study investigates the degree to

0021-9517/84 $3.00

which intraparticle substrate transport influences the activity and selectivity of a transition metal complex catalyst supported on a gel-form, or microporous resin crosslinked polymer An intrinsic polymer-supported reaction regime is established, and kinetic rate parameters are determined The intrinsic rate parameters are incorporated into a mathematical model to describe and predict reaction rates under conditions where intraparticle substrate transport affects the measured rate

Wilkinson's catalyst, $RhCl(PPh_3)_3$, is active for the hydrogenation of olefins at mild conditions (*19*) This complex has been attached to gel-form, polystyrene-divinylbenzene (DVB) polymer beads (*12*), and was selected as the model system for our study The polymer-bound complex retains many features of the homogeneous complex, but alterations in activity and selectivity have been observed (*8 – 16, 20, 21*) Specific changes include reduced activity and lower relative rates of larger substrates, compared to the homogeneous complex Reduced activity and altered selectivity have been attributed to intraparticle substrate mass transfer effects (*8, 9, 11–16*) In addition, the presence of dimers (*22, 23*) and/or multiply chelated rhodium (*16, 20*) may be responsible for the reduced activity

Grubbs *et al* (*13*) measured olefin hydrogenation rates in benzene solution over $RhCl(PPh_3)_3$ supported on 100–200 mesh, polystyrene–2% DVB catalyst beads at 1 0 *M* olefin concentration and 1 atm hydrogen pressure They also measured corresponding hydrogenation rates for the homogeneous complex at 2 5 m*M* $RhCl(PPh_3)_3$ concentrations They observed a decrease in activity for the polymer-bound versus the homogeneous catalyst complex The magnitude of the decrease in activity depended on the olefin molecular size As the olefin size increased, the polymer-bound rate decreased to a greater extent than the corresponding homogeneous rate relative to cyclohexene They proposed that the alteration in selectivity (decreasing relative rate with increasing olefin molecular size) and the decrease in activity for the polymer-bound complex was due to diffusional restrictions within the swollen polymer matrix

The present investigation required numerical values for effective substrate diffusion coefficients as a function of the substrate molecular size and the polymer network morphology We have measured and correlated the diffusion of cyclic hydrocarbons within benzene-swollen, polystyrene–DVB beads in the absence of chemical reaction (*24*) The substrate's diffusion coefficient within the polymer relative to pure solvent, D/D_0, was correlated with the volume fraction of polymer A correlating curve was established for three cyclic hydrocarbons and polymer crosslink densities, and was interpreted in accordance with an accepted model which proposes that the swollen polymer matrix acts as a physical obstruction to diffusion (*25, 26*) These results were used to determine effective substrate diffusion coefficients when the same polymers were used as a support for the transition metal catalyst complex

II METHODS

Catalyst synthesis Wilkinson's catalyst, $RhCl(PPh_3)_3$, was attached to gel-form, polystyrene–(DVB) polymer beads similar to the method employed by Grubbs and coworkers (*13, 21*) Polymer beads which were not previously chloromethylated were washed prior to chloromethylation to remove surface impurities (*27*) The catalyst beads were prepared by chloromethylating the polymer beads with chloromethyl methyl ether (caution high toxicity, potential carcinogen) The chloromethylated polystyrene–DVB was phosphinated by treatment with lithio-diphenylphosphine The rhodium complex was attached to the phosphinated beads by equilibration with Wilkinson's catalyst for at least 5 days This equilibration time should result in uniform distribution of Rh (*21*) All operations

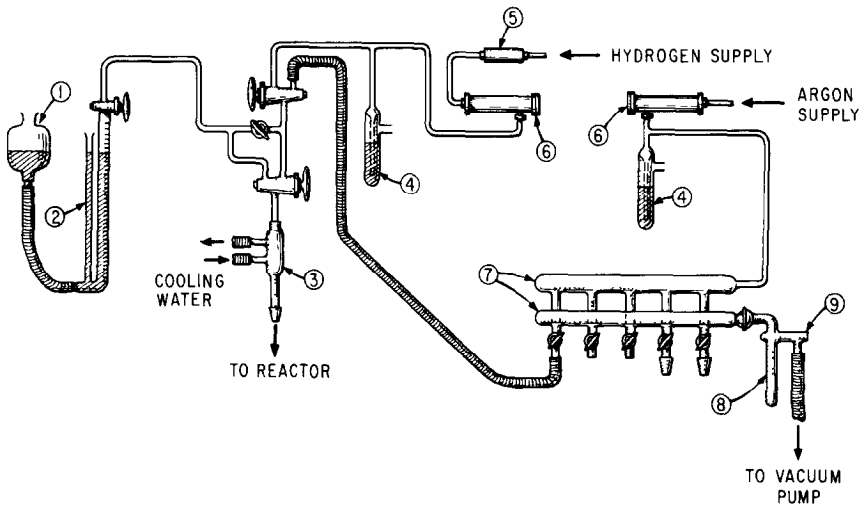

FIG 1 Experimental system schematic 1, Hydrogen buret oil reservoir, 2, hydrogen buret (100 ml), 3, reactor condenser, 4, gas bubbler vent, 5, hydrogen purifier, 6, gas drier, 7, inert gas manifold, 8, liquid nitrogen trap, 9, vacuum gauge

were performed under argon using the inert gas manifold shown in Fig 1 Liquid transfer operations were done using syringe techniques All solvents and reagents were deoxygenated prior to use

Three 200–400 mesh catalyst beads were prepared with crosslink densities of 1, 2, and 3% DVB An 18–20 mesh, 3% DVB catalyst was also prepared The elemental analyses of the phosphinated and catalyst beads as performed by Galbraith Laboratories are presented in Table 1

Catalyst properties Bead swelling ratios, q, defined as the ratio of the benzene-swollen bead volume to the dry bead volume, were determined for the unfunctionalized polymer beads and the catalyst beds according to the procedure used by Roucis and Ekerdt (*24*) These results are presented in Table 1 It was noted that the swelling ratio decreased upon attachment of the rhodium complex relative to the unfunctionalized polymer The swelling ratios of the catalyst beads were measured under argon using oxygen-free benzene and were found not to vary between 25 and 60°C At the low olefin concentrations employed in the hydrogenation studies, approximately

TABLE 1

Polymer-Bound Catalyst Physical Properties

% DVB	Mesh size	wt% P	wt% Cl	wt% Rh	$q_{\text{Polystyrene-DVB}}$	q_{catalyst}
1	200–400[a]	2 82	0 073	—	—	—
	200–400	2 85	—	3 18	6 30	2 51
2	200–400[a]	3 24	0 20	—	—	—
	200–400	3 21	—	3 07	4 03	1 73
3	200–400[a]	2 96	0 22	—	—	—
	200–400	2 95	—	3 20	3 22	1 77
3	18–20[a]	3 07	0 82	—	—	—
	18–20	2 83	—	2 12	3 11	1 60

[a] Analysis of phosphinated polystyrene–DVB prior to complex attachment

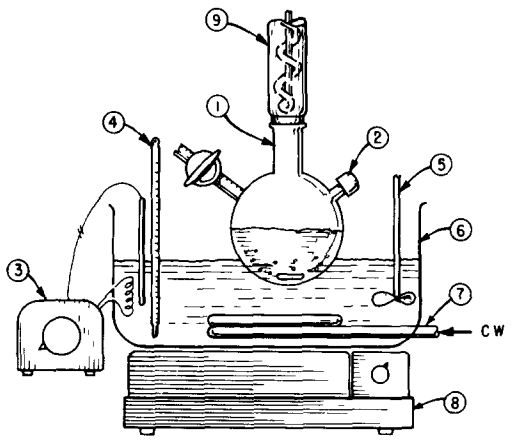

FIG 2 Reactor detail 1, Reactor flask, 2, injection/GC sampling port, 3, constant temperature controller, 4, bath thermometer, 5, bath stirrer, 6, constant temperature bath (oil filled), 7, bath cooling coil, 8, magnetic stirrer (for reactor flask), 9, reactor condenser

0 16 *M* initially, the catalyst bead swelling ratios in the presence of substrate were the same as in the pure benzene solvent

The dry bead density and radius of the 18–20 mesh, 3% DVB catalyst beads were determined experimentally A weighed quantity of catalyst beads was placed in a graduated cylinder and the total bed volume noted The dry catalyst bead density, 1 07 g/cm^3, was then calculated assuming a bed void fraction of 0 44 determined from the unfunctionalized polymer beads A dry catalyst bead radius, 0 0515 ± 0 0096 cm, was determined by photographing bead samples under a microscope Similarly, a dry bead radius of 0 0480 ± 0 0062 cm was determined for the unfunctionalized 18–20 mesh, 3% DVB polymer beads

Partition factors were determined experimentally for the 1, 2, and 3% DVB, 200–400 mesh unfunctionalized beads over the range of substrate concentrations used in the hydrogenation studies The substrate partition factor, K, is defined as the ratio of the equilibrium substrate concentration in the solvent-swollen polymer beads to the substrate concentration in the bulk phase (the solution external to the beads) A weighed quantity of polymer beads was placed in a 50-ml round-bottom flask such that a total swollen bead volume of 23 0 ml resulted after the introduction of 35 0 ml of benzene solvent Cyclohexene was then introduced into the stirred mixture in increments of 0 27 ml until a total of 1 63 × 10^{-2} gmol was injected The bulk phase composition was determined after each injection using a gas chromatograph

Hydrogenation procedure The gas manifold (Fig 1), allowed manipulation of the catalysts under an inert atmosphere Hydrogen was provided to the reactor system by first passing through a Matheson Deoxo filter to remove oxygen impurities, and then through a Matheson Model 460 filter to remove moisture Argon was similarly purified to remove moisture before entering the inert gas manifold The benzene solvent and substrates were distilled over sodium under argon prior to use

The hydrogenation experiments were performed in the reactor system displayed in Fig 1 at 1 atm hydrogen pressure (1 atm equals 101 3 kPa) The reactor detail is presented in Fig 2 The reactor consisted of a 50-ml round-bottom flask equipped with a stopcock sidearm and a rubber septum injection port A water cooled condenser was connected immediately above the reactor The reactor temperature was maintained by an oil bath, and the reactor contents were stirred by a magnetic stirrer

The reduction experiments were performed by first placing a weighed quantity of catalyst into the reactor flask The mass of polymer-bound catalyst used was 3 254 g except for the 3% DVB, 200–400 mesh catalyst bead experiments at 50°C (0 947 g) Homogeneous complex masses necessary to produce a catalyst concentration of 1 00 m*M* were used in the homogeneous reduction experiments

Oxygen was purged from the system by alternate vacuum/hydrogen flushes after the reactor was attached to the hydrogenation system Benzene (16 6 ml for the polymer-bound, and 25 0 ml for the homogeneous reductions) was introduced into the

reactor flask and the catalyst was stirred under hydrogen for at least 1 hr The hydrogen buret was filled with hydrogen and the reactor was brought to the required reaction temperature

The reaction was initiated by injecting a substrate volume corresponding to a total hydrogen uptake of 80 ml (measured at ambient conditions) The time at each 1 ml hydrogen volume interval was recorded as the reaction proceeded to complete conversion The polymer-bound catalysts maintained activity, reaction rates reproduced within 5%

A study was also performed to determine the limiting rate of hydrogen dissolution from the gas phase into the liquid phase during reaction The limiting rate of hydrogen uptake for the system was 1 45 ml H_2/min All reduction rates were kept below this limit

Materials The substrates were reagent grade and purified before use as previously noted The benzene solvent was spectro grade The gases, hydrogen (99 999%) and argon (99 999%) were UHP grade

The homogeneous complex, $RhCl(PPh_3)_3$, was purchased from Strem Chemicals, Inc The 1 and 2% DVB chloromethylated beads were obtained from the Sigma Chemical Company The 3% DVB, 200–400 mesh polymer beads were purchased from Bio-Rad Laboratories The 3% DVB, 18–20 mesh polymer beads were donated by the Dow Chemical Company

III MATHEMATICAL MODEL

In this section, a model is developed which describes simultaneous mass transfer and reaction in solvent-swollen, gel-form polymer catalyst beads The reaction was studied in a batch reactor of total volume V_R, which consists of a solvent-swollen catalyst bead phase and a surrounding bulk phase The substrate diffuses from the bulk phase (of volume V_b) into the catalyst beads (of volume $V_{catalyst}$) as the reaction proceeds

The material balance equation for radial mass transfer and reaction within a spherical catalyst bead was written as,

$$\frac{\partial c}{\partial t} = D\frac{1}{r^2}\frac{\partial}{\partial r}\left(r^2\frac{\partial c}{\partial r}\right) - (-r_s), \qquad (1)$$

where c is the substrate concentration within the swollen catalyst bead, and the effective diffusion coefficient, D, is constant at low substrate concentrations (*24*) The reaction rate term was written as (*13, 16*),

$$(-r_s) = \frac{Ac}{1 + Bc}, \qquad (2)$$

where

$$A = \frac{k' K_{H_2} c_{H_2} n_{Rh}}{1 + K_{H_2} c_{H_2}}, \qquad (3)$$

$$B = \frac{K_s}{1 + K_{H_2} c_{H_2}} \qquad (4)$$

The reaction rate per gram mole of bound rhodium complex was defined as

$$(-r_s)' = \frac{A'c}{1 + Bc}, \qquad (5)$$

where

$$A' = \frac{A}{n_{Rh}} \qquad (6)$$

The kinetic parameters are based on the homogeneous rate expression because the rate expression for polymer-bound Wilkinson's catalyst has been shown (*13, 16, 19*) to be of the same form This correspondence suggested that the mechanism for olefin hydrogenation over polymer-bound Wilkinson's catalyst is the same as the homogeneous complex The hydrogen concentration is assumed constant throughout the catalyst bead since its diffusion coefficient in benzene is more than two times greater than that for cyclohexene (*28*)

Equation (1) in dimensionless form was written as,

$$\frac{\partial \hat{c}}{\partial T} = \frac{1}{R^2}\frac{\partial}{\partial R}\left(R^2\frac{\partial \hat{c}}{\partial R}\right) - \Phi^2\frac{\hat{c}}{1 + B_0\hat{c}}, \qquad (7)$$

where

$$\hat{c}(R,T) = \frac{c(r,t)}{c_{b_0}}, \tag{8}$$

$$T = \frac{Dt}{a^2}, \tag{9}$$

$$a = q^{1/3}\ a_{dry}, \tag{10}$$

$$R = \frac{r}{a}, \tag{11}$$

$$\Phi = a\left[\frac{A}{D}\right]^{1/2} \quad \text{(Thiele modulus)}, \tag{12}$$

$$B_0 = B\ c_{b_0} \tag{13}$$

The substrate concentration at the catalyst surface was related to the surrounding bulk phase concentration by the distribution factor, K, defined as

$$c(a,t) = K\ c_b(t) \tag{14}$$

Equation (7) was solved with the initial conditions,

$$\hat{c}(R,0) = 0, \qquad 0 \le R < 1, \tag{15}$$

$$\hat{c}(1,0) = K, \qquad R = 1, \tag{16}$$

and the boundary condition at the catalyst bead surface,

$$\frac{\alpha}{3}\frac{\partial \hat{c}(1,T)}{\partial T} = -\frac{\partial \hat{c}(1,T)}{\partial R}, \qquad T \ge 0, \tag{17}$$

where

$$\alpha = \frac{V_b}{V_{catalyst}\ K}, \tag{18}$$

$$V_{catalyst} = q\ V_{catalyst,dry} \tag{19}$$

The boundary condition at the catalyst bead surface arose from a material balance on the substrate over the bulk phase, the rate of loss of substrate from the bulk phase is equal to the total flux into the catalyst beads at any time T

The total substrate conversion within the batch reactor, X, was defined in terms of the total moles of substrate present in the reactor at any time T,

$$X(T) = 1 - \frac{n_s(T)}{n_s(0)}, \tag{20}$$

where

$n_s(T)$ = moles substrate in bulk phase + moles of substrate in catalyst beads (21)

The corresponding substrate material balance for the batch reactor gave the total rate of substrate conversion, viz

$$\frac{dX}{dT} = -\gamma\frac{d}{dT}\left\{\left(\frac{\alpha}{\alpha K + 1}\right)\hat{c}(1,T) + \left(\frac{3}{\alpha K + 1}\right)\int_0^1 \hat{c}(R,T)R^2 dR\right\}, \tag{22}$$

where

$$\gamma = \frac{V_R c_{b_0}}{n_s(0)}, \tag{23}$$

$$V_R = V_{catalyst} + V_b \tag{24}$$

The first term in the brackets of Eq (22) corresponds to the moles of substrate in the bulk phase and the second term corresponds to the moles of substrate within the catalyst beads The moles of substrate within the beads were determined by integrating the substrate concentration profile over the bead volume at each time step Equations (7) and (22) were solved numerically using the explicit method

An intrinsic reaction rate is realized when the chemical reaction is rate limiting, implying that the reactant concentration is independent of radial position In the limit that the substrate concentration within the catalyst bead is uniform, the substrate material balance for the batch reactor, Eq (22), reduces to,

$$\frac{dX}{dt} = -\frac{1}{C'(0)}\frac{dC'(t)}{dt} = \frac{A\left(\frac{1}{\alpha + 1}\right)C'(t)}{1 + B\left(\frac{\alpha K + 1}{\alpha + 1}\right)C'(t)}\ \frac{1}{C'(0)}, \tag{25}$$

where

$$C'(t) = \frac{n_s(t)}{V_R} \quad (26)$$

Equation (25) was integrated to give

$$X = 1 - \frac{C'(t)}{C'(0)} = 1 - \exp\left\{-B\left(\frac{\alpha K + 1}{\alpha + 1}\right)[C'(t) - C'(0)] - A\left(\frac{1}{\alpha + 1}\right)t\right\} \quad (27)$$

Equations (25) and (26) represent the conversion rate and conversion at time t for an intrinsic polymer-bound reaction regime, respectively

For a homogeneous complex catalyzed reaction, the catalyst complex occupies the entire solution volume, or $V_b = 0$, therefore $\alpha = 0$ The substrate partition factor, K, is correspondingly unity Equation (25) reduces to

$$\frac{dX}{dt} = -\frac{1}{C'(0)}\frac{dC'(t)}{dt} = \frac{AC'(t)}{1 + BC'(t)}\frac{1}{C'(0)}, \quad (28)$$

which was integrated to give,

$$X = 1 - \frac{C'(t)}{C'(0)} = 1 - \exp\{-B[C'(t) - C'(0)] - At\} \quad (29)$$

Equations (28) and (29) represent the conversion rate and conversion for a homogeneous complex catalyzed reaction

IV RESULTS

A study was completed to determine if intraparticle substrate mass transport limitations influenced the reaction rate for the 200–400 mesh catalyst beads Weisz (*29*) has presented criteria which enable one to establish the influence of intraparticle transport limitations for nth-order heterogeneously catalyzed reactions His criteria use experimentally measured parameters reaction rate, catalyst reactant surface concentration, the effective diffusion coefficient, and the catalyst particle radius For effectiveness factors greater than 95% (less than 5% deviation from a flat concentration profile), the following criteria were given for spherical catalyst particles

$$W_P = \frac{(-r)a^2}{C_0 D} \begin{cases} < 6\ 0 \text{ (zero order)} & (28a) \\ < 0\ 6 \text{ (first order)} & (28b) \\ < 0\ 3 \text{ (second order)} & (28c) \end{cases}$$

The rate expression for olefin hydrogenation, Eq (2), indicates that the reaction order varies from zero order at high olefin concentrations to first order at low olefin concentrations The measured reaction rate was fastest in the zero order regime, therefore, examination of the Weisz parameter, W_P, in the zero order reaction regime gives the most conservative test for possible intraparticle transport limitations

Cyclohexene and cyclooctene hydrogenation rates were measured using the 200–400 mesh catalysts at 25 and 50°C Initial rates were determined from the experimental data for these reactions In determining the diffusion coefficients for the 200–400 mesh catalyst beads, the catalyst bead swelling ratios were used in the correlation developed in Ref *24*, and are presented in Table 2 Swollen particle radii were calculated based on a mean dry bead radius of 0 0028 cm These data and the corresponding Weisz parameters calculated for the 200–400 mesh bead catalyzed reactions are also presented in Table 2 In all cases, the Weisz parameter was at least two orders of magnitude less than the maximum criterion given for the zero order case From these results, it was concluded that the rate data collected for the 200–400 mesh catalysts

TABLE 2

Weisz Parameters for Polymer-Bound Reactions over 200–400 Mesh Catalysts at Initial Conditions

Catalyst %DVB	Substrate	Reactor temp (°C)	D^a (cm²/min) (×10⁴)	a (cm) (×10³)	$\left[\frac{(-r)a^2}{C_0 D}\right]^b$
1	CHX[c]	25 0	22 4	3 78	0 0021
1	COE[d]	25 0	17 4	3 78	0 0023
2	CHX	25 0	4 02	3 34	0 023
2	COE	25 0	3 13	3 34	0 022
3	CHX	25 0	5 81	3 36	0 019
3	COE	25 0	4 52	3 36	0 017
3	CHX	50 0	5 81	3 36	0 060
3	COE	50 0	4 52	3 36	0 051

[a] Calculated using the correlation in Ref *24*
[b] Weisz parameter (W_P)
[c] Cyclohexene
[d] Cyclooctene

represented intrinsic polymer-bound reaction rates

Intrinsic reaction rate parameters, A and B, were calculated by computer fitting (least-squares regression) Eq (27) to the conversion versus time data for the 200–400 mesh bead catalyzed reactions Figures 3 and 4 present the experimental and calculated curves for the reduction of cyclohexene and cyclooctene at 25°C over the 200–400 mesh, 3% DVB catalyst, respectively The polymer-supported intrinsic reaction model, Eq (27), corresponded exactly to the experimental data Intrinsic reaction rate constants and intrinsic reaction model parameters for the hydrogenation of cyclohexene and cyclooctene over the 1, 2, and 3% DVB, 200–400 mesh catalyst beads are presented in Table 3 The reaction rate constants and initial rates measured for the homogeneous complex catalyzed reactions are presented in Table 4 for cyclohexene and cyclooctene reduction at 25°C

The substrate distribution factors K, presented in Table 3, were calculated based on an experimental study which concluded that the substrate distributes uniformly between the swollen-polymer and bulk phases for low DVB-crosslinked polymers The polymer structure should have the greatest influence on partitioning of the substrate Therefore, any thermodynamic partitioning of the substrate due to the presence of bound Rh and polymer-phosphine sites was neglected because of the low metal and phosphine loadings of the catalyst beads

The initial reduction rate of cyclooctene relative to cyclohexene was calculated for each 200–400 mesh catalyst and the homogeneous complex These results are presented in Table 5 The 200–400 mesh, 1% DVB catalyst, which had the largest functionalized swelling ratio, displayed a relative reduction rate similar to the homogeneous complex The 2 and 3% DVB, 200–400 mesh catalysts displayed lower relative reduction rates than the homogeneous complex

Cyclohexene and cyclooctene were also

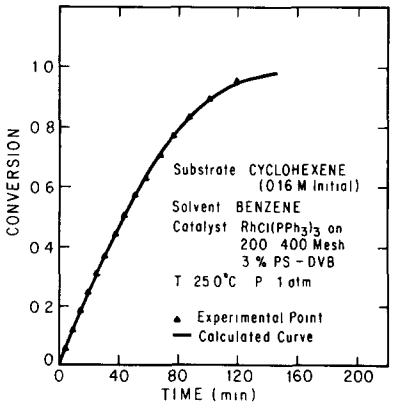

FIG 3 The conversion of cyclohexene versus time in an intrinsic reaction regime

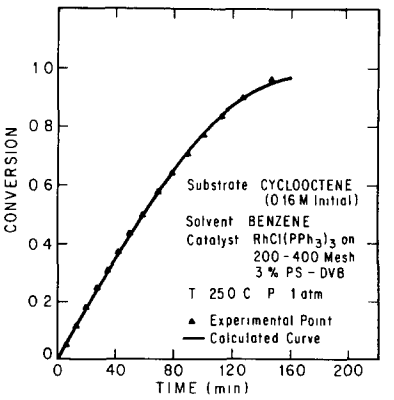

FIG 4 The conversion of cyclooctene versus time in an intrinsic reaction regime

TABLE 3

Polymer-Bound, 200–400 Mesh Catalyst Intrinsic Rate Parameters and Initial Rates

Catalyst % DVB	Substrate	Reactor temp (°C)	K	α	A $(min)^{-1}$	B $(cm^3/gmol)$ $(\times 10^{-4})$	A' $(min\text{-}gmol\ Rh)^{-1}$ $(\times 10^{-2})$	Initial rate gmol substrate / min-cm^3-gmol Rh $(\times 10^3)$
1	CHX[a]	25 0	0 455	2 69	0 214	5 29	2 13	1 52
1	COE[b]	25 0	0 460	2 68	0 268	8 21	2 66	1 29
2	CHX	25 0	0 336	6 62	0 461	7 09	4 75	1 73
2	COE	25 0	0 339	6 62	0 457	10 35	4 70	1 22
3	CHX	25 0	0 346	6 22	0 314	3 30	3 12	2 11
3	COE	25 0	0 348	6 22	0 352	6 41	3 48	1 40
3	CHX	50 0	0 412	23 83	0 686	1 51	23 29	7 79
3	COE	50 0	0 415	23 82	1 825	10 26	61 97	4 93

[a] Cyclohexene
[b] Cyclooctene

hydrogenated over the 18–20 mesh, 3% DVB catalyst at 25 and 50°C Weisz parameters for these experiments are listed in Table 6 The significance of the magnitudes of the Weisz parameters will be discussed in the next section

V DISCUSSION

Intrinsic Reaction Rate Studies

The polymer-supported complex was, in every case, less active than the homogeneous complex on a per gram mole rhodium basis and at similar reaction conditions In the zero order reaction regime, the ratio of the homogeneous to the polymer-bound rate varied between 27 and 37 for cyclohexene hydrogenation at 25°C The polymer-bound complex also displayed different initial reduction rates of cyclooctene relative to cyclohexene, compared to the homogeneous analog

It has been proposed that the reduced activity and altered selectivity may be due to intraparticle substrate transport limitations (*8, 9, 11–16*) The presence of dimers (*22, 23*) and/or multiply chelated rhodium (*16, 20*) may also be responsible for the reduced activity In addition, the alteration in activity and selectivity may be related to the differences in ligand environment between the homogeneous complex and the polymer-supported catalyst Manassen and Dror

TABLE 4

Homogeneous Complex Intrinsic Rate Parameters and Initial Rates at 25°C

Substrate	A $(min)^{-1}$	B $(cm^3/gmol)$ $(\times 10^{-4})$	A $(min\text{-}gmol\ Rh)^{-1}$ $(\times 10^{-2})$	Initial rate gmol substrate / min-cm^3 gmol Rh $(\times 10^3)$
CHX[a]	0 0737	4 22	28 41	56 48
COE[b]	0 0242	1 22	9 33	45 67

[a] Cyclohexene
[b] Cyclooctene

TABLE 5

Initial Reduction Rates of Cyclooctene Relative to Cyclohexene at 25°C

Catalyst support	Catalyst bead swelling ratio (q)	Initial relative rate
Homogeneous complex	—	0 81
1% DVB/200–400 mesh	2 51	0 85
2% DVB/200–400 mesh	1 73	0 71
3% DVB/200–400 mesh	1 77	0 66
3% DVB/18–20 mesh[a]	1 60	0 58

[a] Based on measured rate (not intrinsic activity)

TABLE 6

Model Simulation Input Parameters and Weisz Parameters for the Hydrogenation of Cyclohexene and Cyclooctene over 18–20 mesh, 3% DVB Catalyst Beads

Substrate	Reaction temp (°C)	α	K	a (cm)	D (cm^2/min) ($\times 10^5$)	A (min^{-1})	Φ	B_0	W_P
CHX[a]	50	8 27	0 301	0 0602	2 98	1 56	13 78	22 39	16 6
COE[b]	50	8 27	0 303	0 0602	2 32	4 15	25 47	27 27	17 9
CHX	25	8 27	0 301	0 0602	2 98	—	—	—	3 7
COE	25	8 27	0 303	0 0602	2 32	—	—	—	3 5

[a] Cyclohexene
[b] Cyclooctene

(*10*) report the effect on homogeneous activity due to alteration of the substituents on one of the phenyl rings of the triphenylphosphine ligand They also reported the effect of the P/Rh ratio on the activity of the homogeneous complex (*10*) The activity decreased with P/Rh ratios greater than 2 2–2 3, but the degree of decrease was dependent upon ligand structure The influence of intraparticle transport on the activity and selectivity of the polymer-bound catalyst complex is discussed below

Activation energies for the 3% DVB, 200–400 mesh catalyst were estimated for cyclohexene, 10 0 kcal/gmol, and for cyclooctene, 9 6 kcal/gmol, from initial rate data at 25 and 50°C The activation energy for cyclohexene hydrogenation is consistent with the value reported by De Croon and Coenen (*16*) for a similar catalyst, 11 7 kcal/gmol (Polystyrene–2% DVB phosphinated in the same manner presented in the Methods section, with a Rh loading of 8 82 wt% and a bead diameter of 0 46 μm) They found that the homogeneous complex displays an activation energy of 22 kcal/gmol for cyclohexene hydrogenation

In general, when the activation energy decreases by a factor of two in heterogeneous systems, severe mass transfer limitations are responsible (*30*) De Croon and Coenen proposed that intraparticle substrate transport effects explained the large apparent decrease in activation energy Using the data presented in their paper (*16*) and accounting for differences in substrate concentration and polymer bead metal loading, we estimate a Weisz parameter of order 10^{-5} A value of the effective diffusion coefficient (*24*) was determined for this calculation based on the functionalized swelling ratio we determined from a similar catalyst ($D \sim 2 \times 10^{-5}$ cm^2/min) The value of the Weisz parameter given above suggests that De Croon and Coenen were also observing intrinsic rate phenomena Since we have determined that intraparticle substrate transport limitations were negligible for cyclohexene and cyclooctene within the 200–400 mesh catalysts studied, the activation energies we have calculated are intrinsic The present results and De Croon and Coenen's results demonstrate that the activity of the polystyrene-supported complex is inherently different than the homogeneous catalyst

Hydrogenation rates for cyclohexene and cyclooctene were measured by Grubbs *et al* (*13*) over $RhCl(PPh_3)_3$ supported on 100–200 mesh, polystyrene–2% DVB polymer beads They reported a relative initial rate of 0 39 for cyclooctene relative to cyclohexene They found a similar relative rate of unity for the homogeneous complex They proposed that the slower diffusion of the larger substrate molecule (cyclooctene) within the swollen polymer matrix was responsible for the lower relative rate of the

bound catalyst compared to the homogeneous complex Based on data presented in their paper (*13*), we estimate a Weisz parameter of order 10^{-2} for both cyclohexene and cyclooctene hydrogenation over their catalyst beads This calculation suggested that Grubbs *et al* were also observing intrinsic polymer-supported reaction rates under the conditions they studied Lower relative reduction rates compared to the homogeneous complex may be due to alteration of the ligand environment (*9, 10*) as previously discussed, or to steric constraints imposed by the presence of the polymer support in the vicinity of active rhodium

Our studies also indicated a lower reduction rate of cyclooctene relative to cyclohexene for the 2 and 3% DVB, 200–400 mesh catalysts compared to the corresponding homogeneous relative rate Although it may be inappropriate to compare relative rates between the homogeneous and polymer-supported complex, relative reduction rates for polymer-supported catalysts may be compared since the rhodium complexes are in similar ligand environments A greater polymer chain density would be expected to increase steric constraints due to increased crowding in the vicinity of the bound complex sites The polymer chain density increases as the functionalized swelling ratio decreases The relative rate for the 1% DVB, 200–400 mesh catalyst was greater than either the 2 or 3% DVB, 200–400 mesh catalysts, which displayed similar relative rates and functionalized swelling ratios The swelling ratio of the 1% DVB catalyst was greater than either the 2 or 3% DVB catalysts These results indicate that the intrinsic activity of polymer-bound catalysts is related to the functionalized swelling ratio

The bead swelling ratio, q, was found to decrease upon fixation of the rhodium complex as shown in Table 1 Since the swelling ratio decreased relative to the unfunctionalized polymer, the rhodium complex within the catalyst beads may be in a dimer form (*22, 23*), or attached to the polymer through more than one polymer–phosphine ligand (*16, 20*) The observed decrease in activity of the polymer-bound complex compared to the homogeneous complex may be due to the substantial presence of these complex forms

In order to investigate the nature of the polymer-bound complex, the elemental analyses, Table 1, were used to estimate the mole ratio of triphenylphosphine to rhodium, PPh_3/Rh, for each of the 200–400 mesh catalysts The ratios were calculated by assuming that the number of polymer–phosphine groups per gram of polymer support remained constant after the catalyst was attached to the phosphinated polymer The PPh_3/Rh ratios determined by this procedure produced an average of 0 18 ± 0 003 The mole ratio of total phosphorus to rhodium, P/Rh, was in the range of 3 0–3 5 for these three catalysts

Reed *et al* (*22*) observed a dimeric structure for $RhCl(PPh_3)_3$ bound to 2% polystyrene–DVB functionalized with the same polymer–phosphine structure used in this study The dimer had one triphenylphosphine and one polymer–phosphine per rhodium atom If the rhodium complex is primarily in the dimer form, a PPh_3/Rh ratio near unity would be observed The mononuclear complex is expected to have three phosphine ligands (*19*) The fact that the observed PPh_3/Rh ratio was less than unity for each polymer-bound catalyst suggests that a substantial number of rhodium complexes are bound to the polymer through more than one polymer–phosphine ligand

The initial reduction rate per gram mole of polymer-bound rhodium complex was found in general to increase as the divinylbenzene content of the 200–400 mesh, polystyrene–DVB polymer support increased Lower polymer crosslink densities produce a more mobile structure in the solvent-swollen state If complex dimerization or multiple chelation of the rhodium complex to the polymer support results in inactive, or less active rhodium, a more mobile poly-

mer structure would facilitate their formation Therefore, higher polymer crosslink densities should produce somewhat more isolated complex coordination sites This effect, in addition to the effect of increasing solvent-swollen structure rigidity with increasing polymer DVB content, may explain the observed increase in activity with increasing polymer DVB content

Intraparticle Mass Transfer Effects

The mathematical hydrogenation model was developed to describe simultaneous diffusion and reaction in a gel-form, polymer-bound rhodium catalyst Development of the model revealed the physical and chemical variables needed to predict polymer-bound catalyst activity The parameters needed to characterize this reaction system include the effective diffusion coefficient, D, the substrate partition factor, K, and the intrinsic rate parameters, A and B These parameters were measured independently and were used in the model to predict the observed substrate conversion rate for an intraparticle mass transfer influenced reaction

In order to apply the model, a catalyst support and reaction regime were chosen such that substrate transport limitations would influence the reaction rate Wilkinson's catalyst was attached to large diameter polystyrene–DVB beads, 18–20 mesh, 3% DVB A reaction temperature of 50°C was chosen because it resulted in a relatively fast reaction rate without introducing further complications such as severe solvent loss from the liquid phase (bp benzene at 1 atm = 80°C)

The dependence of the diffusion coefficients on the polymer swelling ratio demonstrated that the crosslinked polymer network acted as a physical obstruction to solute transport (*24*) In determining diffusion coefficients for the catalyst beads, the suggested presence of dimers or multiple polymer–phosphine chelation was assumed to act as further crosslinking agents The catalyst bead swelling ratio was used to calculate the effective diffusion coefficients for the 18–20 mesh catalyst simulations at 25°C Since the activation energy for diffusion is low (*31*), the diffusion coefficients calculated at 25°C were assumed the same at 50°C The numerical values calculated for the diffusion coefficients are presented in Table 6 Substrate distribution factors, K, were calculated for the 18–20 mesh catalyst based on uniform substrate distribution, as previously discussed, and are also presented in Table 6

Examination of the Weisz parameter for the 18–20 mesh catalyst hydrogenations (Table 6) revealed that the reaction rate was influenced by intraparticle substrate mass transfer between 25 and 50°C Although the Weisz parameters calculated for a reaction temperature of 25°C were less than six (3 7 for cyclohexene and 3 5 for cyclooctene), Butt (*32*) recommends that marginal satisfaction Weisz's criteria not be used He recommends that Weisz's criteria be satisfied by at least an order of magnitude in order to be certain that intraparticle transport effects are negligible compared to the intrinsic reaction rate For this reason, the rate data collected for the 18–20 mesh catalyst hydrogenations could not be used to determine intrinsic reaction rate parameters In addition, mechanical reduction of the 18–20 mesh catalyst beads was not possible due to the high elasticity of the low DVB-crosslinked polymer The highly air sensitive nature of the polymer-supported catalyst prevented bead size reduction by other means

Intrinsic activity was shown earlier to be related to the polymer support DVB content The intrinsic reaction rate parameters, A and B, for the 3% DVB, 18–20 mesh catalyst simulations were determined from the 3% DVB, 200–400 mesh catalyst reaction data Both catalysts were synthesized using identical procedures, and reaction rate parameters were determined under the same reaction conditions The 18–20 mesh, 3% DVB catalyst had a larger total P/Rh ratio

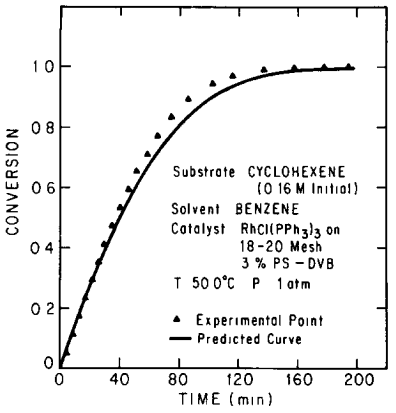

FIG 5 The conversion of cyclohexene versus time over the 18–20 mesh catalyst beads

than the 3% DVB, 200–400 mesh catalyst It was not possible to adjust the intrinsic rate constants for the different P/Rh ratios, nor determine the magnitude of the effect, if any However, the rate parameter A, which contains the effective number of active sites per gram of catalyst, was corrected for the difference in rhodium loadings The parameter, B, was assumed to be the same for both catalysts since it contains only equilibrium constants (Eq (4))

The numerical values of the physical and chemical parameters used to simulate the performance of the 18–20 mesh, 3% DVB catalyst for hydrogenation of cyclohexene and cyclooctene at 50°C are listed in Table 6 The predicted curve of conversion versus time and the experimental data are presented in Fig 5 for cyclohexene, and in Fig 6 for cyclooctene

The mathematical model predicted the experimental data for the hydrogenation of cyclohexene This correspondence infers that the controlling physical and chemical variables needed to characterize simultaneous mass transfer and reaction for this catalyst system were properly identified and measured An effectiveness factor of 0 43 was calculated at zero time, and a Weisz parameter of 16 6 was calculated These results indicate that intraparticle mass transport influenced the reaction rate for this catalyst under these reaction conditions

The intrinsic rate parameters described the intrinsic activity of the 18–20 mesh catalyst for cyclohexene reduction The difference in the functionalized swelling ratios and the total P/Rh between the 200–400 and 18–20 mesh, 3% DVB catalysts did not have a significant effect on intrinsic activity for cyclohexene as a substrate This could be due to the fact that the total P/Rh ratio includes uncoordinated polymer–phosphine

Application of the intrinsic reaction rate parameters determined from cyclooctene hydrogenation data over the 200–400 mesh, 3% DVB catalyst in the mathematical model predicted a reaction rate higher than that observed The functionalized swelling ratio for the 200–400 mesh, 3% DVB catalyst was greater than the 18–20 mesh catalyst As previously discussed, the steric hindrance effects of the polymer network on catalyst activity increase with decreasing functionalized swelling ratios This effect should become more apparent for larger substrate molecular sizes Therefore, the intrinsic rate parameters calculated from the 200–400 mesh, 3% DVB catalyst reductions, may have overestimated the intrinsic reaction rate for cyclooctene reduc-

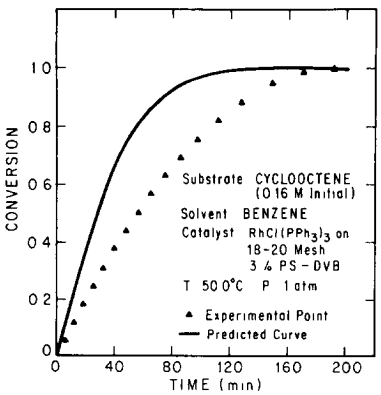

FIG 6 The conversion of cyclooctene versus time over the 18–20 mesh catalyst beads

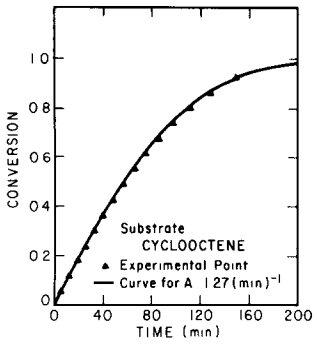

FIG 7 Calculated curve of cyclooctene conversion versus time for $A = 1\ 27\ min^{-1}$

tion over the 18–20 mesh, 3% DVB catalyst beads

A study was completed to determine if the discrepancy between the experimental data and the predicted curve for cyclooctene was in fact due to difficulties in extrapolating the intrinsic rate parameter, A, determined from the 200–400 mesh, 3% DVB catalyst to the 18–20 mesh catalyst Various values of A were inserted into the mathematical hydrogenation model until an optimum fit to the experimental data was achieved This optimum fit occurred for a value of A equal to $1\ 27\ min^{-1}$

The overprediction of the reaction rate for cyclooctene was also studied to determine if it was related to errors in the effective diffusion coefficient A value of the diffusion coefficient which corresponded to the maximum relative uncertainty in the diffusion coefficient (12%) was inserted into the mathematical hydrogenation model The predicted reaction rate was negligibly reduced (5%) using this lower value for the diffusion coefficient

The calculated curve of cyclooctene conversion versus time using a value of A equal to $1\ 27\ min^{-1}$ and the experimental data are presented in Fig 7 The hydrogenation model corresponded precisely to the experimental data when this value of the rate parameter, A, was inserted into the model with all other variables unchanged The mathematical model, Eq (22), is therefore consistent with the experimentally observed reaction rate when intraparticle mass transport effects are present Ideally, the intrinsic activity should be determined using fine-mesh catalyst beads which are physically and chemically identical to the large diameter catalyst beads

The prediction of intraparticle mass transport limitations within a gel-form, or microporous polymer-supported catalyst system is consistent with the effective diffusion model presented in our earlier paper (*24*) A minimum number of variables are needed to characterize the activity of the polymer-supported catalyst system, and may be determined independently This feature should allow the approach used herein to be applied to other gel-form, polymer-supported catalyst systems

SUMMARY

A mathematical model was developed and used to investigate simultaneous mass transfer and reaction within a polystyrene–DVB supported rhodium catalyst Development of the model revealed the physical and chemical variables needed to characterize this catalyst system These variables include the effective diffusion coefficient of the substrate, a partition factor which relates the thermodynamic partitioning of the substrate between the solvent-swollen catalyst bead and the bulk phase, and the intrinsic reaction rate parameters needed in the kinetic expression

The substantial activity decrease observed upon attachment of $RhCl(PPh_3)_3$ to polystyrene–DVB was not due to intraparticle mass transport limitations Changes in the rate of cyclooctene reduction relative to cyclohexene are not caused by differences in intraparticle diffusion rates The selectivity of the polymer-bound catalyst complex appears to be related to the swelling ratio implying that steric constraints due to the presence of the polymer support in the vicinity of active rhodium affect activity The intrinsic polymer-bound activity was found

to increase with polymer crosslink density An observed decrease in the swelling ratio upon catalyst attachment, and calculations of the ratio of triphenylphosphine to rhodium, indicated multiple polymer–phosphine chelation The presence of multiply chelated rhodium may account for the lower activity relative to the homogeneous complex

NOMENCLATURE

a	Solvent-swollen catalyst bead radius (cm)
a_{dry}	Dry catalyst bead radius (cm)
A	Intrinsic reaction rate parameter (min^{-1})
A'	Intrinsic reaction rate parameter per gram mole Rh (min^{-1} gmol Rh^{-1})
B	Intrinsic reaction rate parameter (cm^3/gmol)
B_0	Intrinsic reaction rate parameter (dimensionless)
$c(r,t)$	Substrate concentration within solvent-swollen catalyst bead (gmol/cm^3)
c_{b_0}	Initial bulk phase substrate concentration (gmol/cm^3)
$c_b(t)$	Bulk phase substrate concentration (gmol/cm^3)
c_{H_2}	Hydrogen concentration (gmol/cm)
$\hat{c}(R,T)$	Dimensionless substrate concentration within solvent-swollen catalyst bead
$C'(t)$	Superficial substrate concentration within total reactor volume (gmol/cm^3)
D	Effective substrate diffusion coefficient (cm^2/min)
k'	Rate constant (min^{-1})
K	Substrate partition (distribution) factor (dimensionless)
K_{H_2}	Equilibrium constant, hydrogen (cm^3/gmol)
K_s	Equilibrium constant, substrate (cm^3/gmol)
n_{Rh}	Total moles of polymer-bound rhodium (gmol)
$n_s(T)$	Total moles of substrate within reactor (gmol)
q	Bead swelling ratio (swollen vol/dry bead vol)(dimensionless)
r	Radial coordinate (cm)
$(-r)$	Reaction rate (gmol substrate/min-cm^3 catalyst)
$(-r_s)$	Reaction rate (gmol substrate/min-cm^3)
$(-r_s)'$	Reaction rate per mole of polymer-bound rhodium (gmol substrate/min-cm^3-gmol Rh)
R	Dimensionless radial coordinate
t	Time (min)
T	Dimensionless time
V_b	Bulk phase volume (cm^3)
$V_{catalyst}$	Total solvent-swollen catalyst volume (cm^3)
$V_{catalyst,dry}$	Total dry catalyst volume (cm^3)
V_R	Total reactor volume (cm^3)
W_P	Weisz parameter defined by Eq (28) (dimensionless)
X	Substrate conversion (dimensionless)
α	Parameter defined by Eq (18) (dimensionless)
γ	Parameter defined by Eq (23) (dimensionless)
Φ	Thiele modulus (dimensionless)

ACKNOWLEDGMENT

This work was supported by the Dow Chemical Company, Midland, MI

REFERENCES

1 Murrell, L L , *in* "Advanced Materials in Catalysis" (J J Burton, and R L Garten, Eds) Academic Press, New York, 1977
2 Yermakov, Y I , *Cat Rev -Sci Eng* **13,** 77 (1976)
3 Pittman, C U , and Evans, G O , *CHEMTECH* Sept , 560 (1973)
4 Heinemann, H , *CHEMTECH* May, 286 (1971)
5 Bailer, J C , Jr , *Cat Rev -Sci Eng* **10,** 17 (1974)

6 "Polymer-supported Reactions in Organic Synthesis" (P Hodge and D C Sherrington, Eds) John Wiley, New York, 1980

7 Collman, J P , and Hegedus, L S , "Principles and Applications of Organotransition Metal Chemistry " University Science Books Mill Valley, California, 1980

8 Ciardelli, F , Braca, G , Carlini C , Sbrana G and Valentini, G , *J Mol Catal* **14,** 1 (1982)

9 Strukul, G , D'Olimpio, P , Bonevento, N , Pinna, F , and Graziani, M , *J Mol Catal* **2,** 179 (1977)

10 Manassen, J , and Dror, Y , *J Mol Catal* **3,** 227 (1977/78)

11 Pittman, C U , Smith, L R , and Hanes, R M , *J Amer Chem Soc* **97,** 1742 (1975)

12 Grubbs, R H , and Kroll, L C , *J Amer Chem Soc* **93,** 3062 (1971)

13 Grubbs, R H , Kroll, L C , and Sweet, E M *J Macromol Sci -Chem* **A7,** 1047 (1973)

14 Gayot, A , Graillat, CH , and Bartholin, M , *J Mol Catal* **3,** 39 (1977/78)

15 Whitehurst, D D , *CHEMTECH* January, 44 (1980)

16 De Croon, M H J M , and Coenen, J W E , *J Mol Catal* **11,** 301 (1981)

17 Dooley, K M , Williams, J A , Gates, B C , and Albright, R L , *J Catal* **74,** 361 (1982)

18 Diemer, J , R B , Dooley, K M , Gates, B C , and Albright, R L , *J Catal* **74,** 373 (1982)

19 Osborn, J A , Jardine, F H , Young, J F , and Wilkinson, G , *J Chem Soc* **(A),** 1711 (1966)

20 Grubbs, R H , Gibbons, C , Kroll, L C , Bonds, W D , and Brubaker, C H , *J Amer Chem Soc* **95,** 2373 (1973)

21 Grubbs, R H , and Sweet, E M , *J Mol Catal* **3,** 259 (1977/78)

22 Reed J Eisenberger, P Teo, B K and Kincaid, B M *J Amer Chem Soc* **99,** 5217 (1977)

23 Reed, J , Eisenberger P , Teo, B K , and Kincaid, B M , *J Amer Chem Soc* **100,** 2375 (1978)

24 Roucis, J B , and Ekerdt, J G *J Appl Polym Sci* **27,** 3841 (1982)

25 Mackie, J S , and Meares, P , *Proc Roy Soc London* **A232,** 498 (1955)

26 Meares, P , *J Polym Sci* **20,** 507 (1956)

27 Relles, H M , and Schluenz, R W , *J Amer Chem Soc* **96,** 6469 (1974)

28 Reid, R C , Prausnitz, J M , and Sherwood, T K *in* "The Properties of Gases and Liquids " McGraw-Hill, New York, 1977

29 Weisz, P B *Z Phys Chem N F* **11,** 1 (1957)

30 Petersen, E E , *in* 'Chemical Reaction Analysis " Prentice Hall, Englewood Cliffs, New Jersey, 1965

31 Muhr, A H , and Blanshard, J M V , *Polymer* **23,** 1012 (1982)

32 Butt, J B , *in* "Reaction Kinetics and Reactor Design " Prentice Hall, Englewood Cliffs, New Jersey, 1980